Investigating the role of thermal stresses on induced seismicity

Kyungjae Im[*] and Jean-Philippe Avouac, Geology and Planetary Science Division, California Institute of Technology

Summary
We investigate the influence of thermal stresses on induced seismicity in the context of geothermal energy production at Brawley and Coso in California. We resort to thermo-hydro-mechanical modeling and used measurements of surface deformation to validate our simulations. We find that thermal stresses induced by fluid injections for geothermal energy production play an important role in either triggering or impeding seismicity. We speculate that thermal stresses may also play an important role in inducing fracturing and seismicity in other context of fluid injection for CO2 storage, disposal of wastewater or unconventional oil and gas production for example.

Introduction
There is much need in understanding better how seismicity relates to geo-energy production, whether fossil fuels or geothermal energy. Induced and triggered earthquakes have indeed been an impediment to the development of Enhanced Geothermal Systems for geothermal energy production. In addition, there is rising concern and only limited understanding regarding the hazard posed by injection of wastewater from unconventional oil & gas production [*Ellsworth*, 2013; *Elsworth et al.*, 2016; *Goebel et al.*, 2017; *Goebel and Brodsky*, 2018; *Grigoli et al.*, 2018; *Kim et al.*, 2018]. In these contexts, thermal stresses may play an important role [Candela et al., 2018]. We have therefore investigated in more depth the relationship between seismicity and effective stress variations due to poro-elastic and thermal effects focusing on geothermal energy production sites at Brawley and Coso in California.

Induced seismicity related to geothermal operations at Coso and Brawley, California.
We analyzed seismicity and deformation related to the Brawley and Coso geothermal plants in California. An intense seismic crisis occurred in 2012 at Brawley, including a Mw 5.4 earthquake, which started over two years after the onset of energy production (Figure 1). Analysis of InSAR and geodetic data revealed that this earthquake was preceded and triggered by aseismic motion of a normal fault [*Wei et al.*, 2015]. The inversion revealed clearly that the zone of aseismic slip correlates with the zone of fluid injection (Figure 1c). This inversion assumes that slip on the normal fault was the sole cause of the measured surface deformation. Clearly, thermal contraction must also have contributed. It is actually probable that both pore pressure increase in the fault zone and unclamping by thermal contraction stresses contributed to activating this fault.

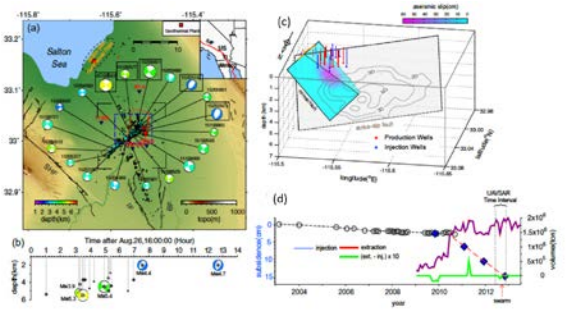

Figure 1: The 2012 Brawley swarm [figures from *Wei et al.*, 2015]. (a) Seismicity (black circles) recorded from 26 Aug. 2012 to 26 Sept. 2012. The blue dashed rectangle outlines the region shown in (c). (b) Depths and M>3.5 events during the swarm. (c) 3-D view of slip on faults and injection/production wells. Aseismic slip distribution on the normal fault is color coded, and the slip due the two strike-slip events (Mw5.3 and Mw5.4) is shown as contour lines. Production (red) and injection (blue) wells. The orange line shows the surface rupture of the Mw4.7 earthquake revealed by the UAVSAR data. (d) Subsidence history. Black circles are derived from InSAR and blue diamonds from leveling. Monthly injection (thin, blue) and production (heavy, blue) volumes; the difference between injection and production volume is very small (green).

Large-scale geothermal power production at Coso (Figure 2) started in 1987 with an electrical power capacity of over 250MW, triggering an intense increased of seismicity. The seismicity rate peaked between 1995 and 2000 and decreased gradually later on. The Coso geothermal field lies just North of the ruptures of the 2019 Ridgecrest earthquakes. A striking feature of the distribution of aftershocks is the lack of aftershocks within the geothermal field area (triangles show location of geothermal wells in Figure 2) where the static Coulomb stress increased as a result of the mainshocks. This observation is surprising as hydrothermal areas are known to be prone to remote triggering [*e.g., Hill, 1993; Brodsky and Prejean, 2005*] and that geothermal operations are known to trigger earthquakes [*e.g., Deichmann and Giardini, 2009; Grigoli et al., 2018; Kim et al., 2018*]. This observation is however consistent with a previous investigation which revealed a lack of remote triggering in that same area [*Zhang et al, 2018*]. Thermal stresses evolve slowly, and as they accumulate, they can eventually become significant and result in failure and reduction of the deviatoric stresses [*Im et al., 2017*].

Subsidence exceeding 14 cm between September 1993 and June 1998 was measured using SAR interferometry over the injection area [*Fialko and Simons, 2000*] and was most

likely driven by thermal contraction as commonly observed over other geothermal fields [*Mossop and Segall, 1997*]. We thus hypothesize that the cumulated stress changes induced by geothermal heat production at Coso since 1987 initially drove an increased of seismicity but impeded earthquake triggering during the Ridgecrest earthquake sequence of 2019.

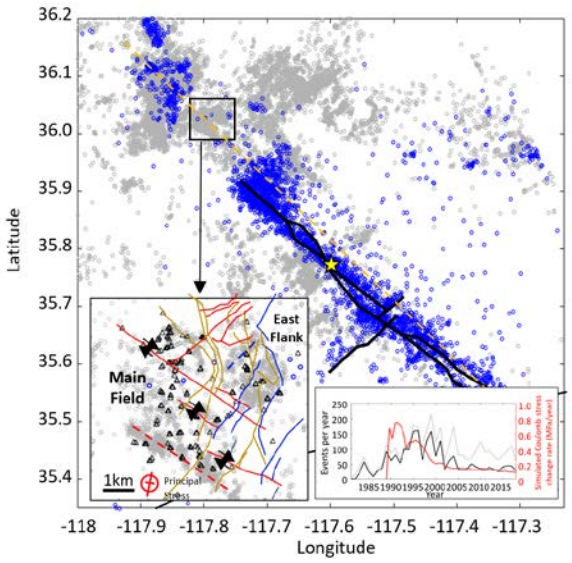

Figure 2: Seismicity before and after the 2019 Mw 7.1 Ridgecrest mainshock. Blue circles denote 20 days of aftershocks (M>2; USGS, earthquake.usgs.gov), yellow star denotes epicenter of M7.1 earthquake, black line denotes fault geometry of Ridgecrest earthquakes [*Ross et al., 2019*], gray circles denote relocated seismicity during 1981 – 2017 (M>1) [*Hauksson et al., 2012*]. Bottom left inset**:** zoomed-in view of the Coso geothermal field. Solid lines represent identified faults [*Davatzes and Hickman, 2006*], dashed lines denote example of fault expressed by seismic clouds and triangles denotes geothermal well locations (maps.conservation.ca.gov/doggr). Bottom right inset: Seismicity rate variations and Coulomb stress rate at the center of the reservoir due to thermal contraction and brittle failure of the reservoir compared with seismicity rate around Coso.

Method

We modeled the thermo-hydro-mechanical response of both systems using Tough-FLAC [*Taron et al., 2009*; *Rutqvist*, 2011] (Figures 3).

Figure 3 shows for example the model set up for the Coso (a) and Brawley (b) simulations. The elements are divided into reservoir, host and fault (Brawley only) block. All elements are assigned with a volumetric thermal contraction coefficient 4.5×10^{-5} /K [*Cooper and Simmons, 1977*], bulk modulus of 20GPa and Poisson's ratio of 0.2. Reservoir elements (blue blocks) are embedded at depth between 1km ~ 3km, assumed to fail according to the Mohr-Coulomb criteria with a friction coefficient of 0.6 and cohesion 2MPa for reservoir and 0 for fault elements, while host rock elements are (green blocks) fully elastic.

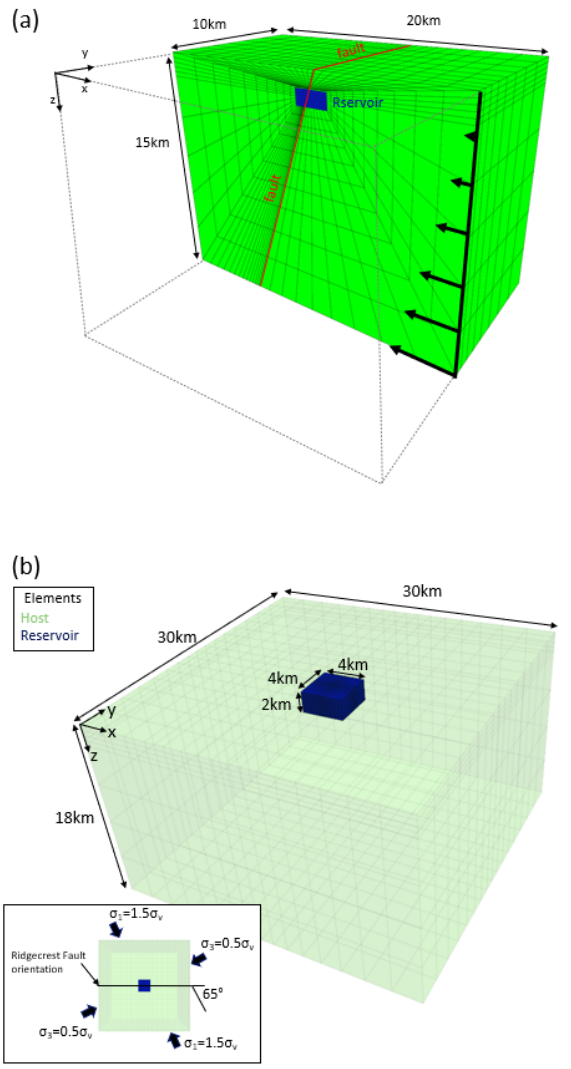

Figure 3: (a) Brawley scale simulation model. (b): Coso scale simulation model. Blue and green blocks represent reservoir and host elements respectively. Inset: Initial horizontal stresses, which are calculated based on the Coso field data (Fig. 2 inset). In both simulations 5-spot pattern of injectors and producers applied at two depths within the reservoir. Unlike the Coso simulation (b), Brawley simulation (a) incorporates normal fault (red) across the reservoir and host rock.

Role of Thermal Stresses on Induced Seismicity

Simulation Results

Both Brawley (Figure 4a) and Coso (Figure 4b) cases show strong Coulomb stress increase within the reservoirs, indicating that seismicity can be induced. Indeed, when a normal fault is incorporated in the model (i.e. Brawley simulation; figure 4a), the fault is reactivatied and slip reaches to the surface. This surface rupture, together with thermal contraction induces strong surface subsidence at the surface (Figure 4a inset). Significant surface subsidence consistent with our modeling results is actually observed at Coso [*Fialko and Simons, 2000*] and at Brawley [*Wei et al., 2015*], with indication of surface faulting in that case as predicted by our model.

Strong negative Coulomb stress are observed in the surrounding area of the depleted reservoir due to the development of compressive circumferential stress [*Segall and Fitzgerald, 1998*]. However, in Brawley case (figure 4a), a zone of strong positive Coulomb stress change is predicted below the reservoir (Figure 4a). This is because of the stress transfer due to the fault reactivation. This result illustrates how the thermal stress change at shallower reservoir can be transferred to deep through the aseismic fault reactivation.

Our Coso field simulation predicts a cumulative surface subsidence of ~30cm over 30 years across an area generally consistent with the subsidence measured from InSAR [*Fialko and Simons, 2000*]. According to our model, the Coulomb stress on a fault parallel to the Ridgecrest rupture increased by as much as 13MPa due to thermal contraction of the reservoir (Fig. 4b). This strong Coulomb stress change can lead to near complete shear stress depletion. This mechanism can explain the lack of aftershocks following the 2019 Ridgecrest earthquake, the lack of remotely triggered earthquakes in recent years [*Zhang et al., 2017*].

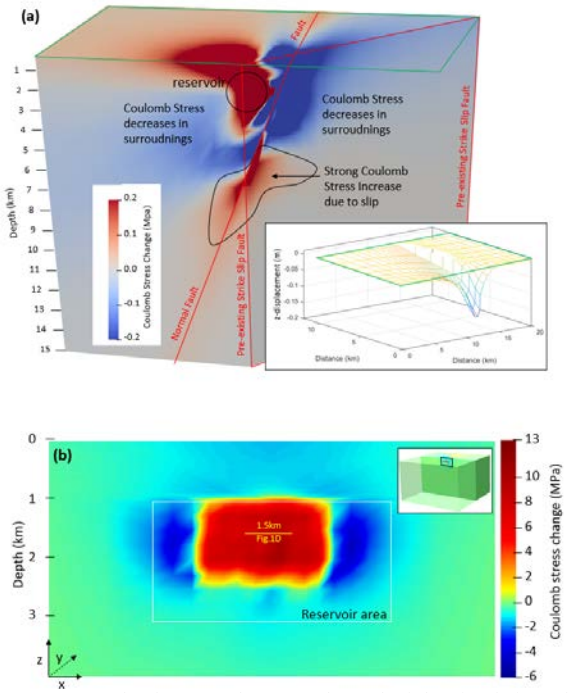

Figure 4: Coulomb stress change at the end of the simulation of Brawley simulation (a) and Coso simulation (b). Coulomb stress change is evaluated in the orientation of Mw 5.3 Brawley earthquake (red rectangle in a), and Mw 7.1 Ridgecrest earthquake (xz plane in b). Inset in (a) show surface deformation induced by both thermal subsidence and fault reactivation and surface rupture.

Conclusion

We conclude that thermal stresses induced by fluid injections for geothermal energy production play an important role in either triggering or impeding seismicity. We speculate that thermal stresses may also play an important role in inducing fracturing and seismicity in other context of fluid injection for CO2 storage, disposal of wastewater or unconventional oil&gas production for example.

Acknowledgement

This study was supported partly by the NSF/IUCRC Geomechanics and Mitigation of Geohazards and by the National Science Foundation via the Southern California Earthquake Center.